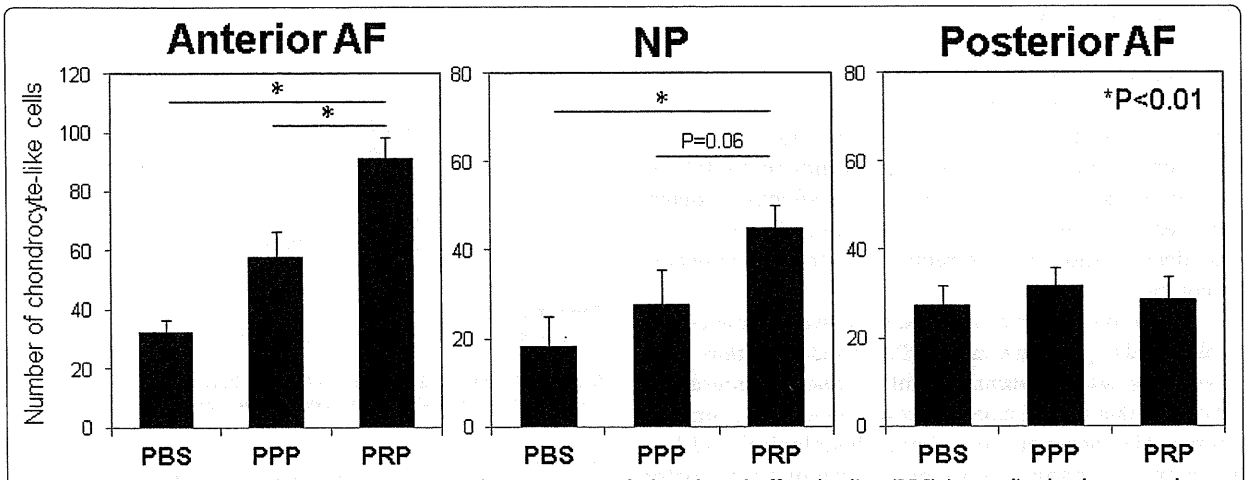

Figure 6 The number of chondrocyte-like cells after injections of phosphate-buffered saline (PBS) (control), platelet-poor plasma (PPP)-releasate, or platelet-rich plasma (PRP)-releasate. The numbers of chondrocyte-like cells in the inner anterior and posterior anulus fibrosus (AF) and the center of the nucleus pulposus (NP) were manually counted by using light microscopy. In the anterior AF, the number of chondrocyte-like cells in the PRP group was significantly higher than those of the PBS and PPP groups (P <0.01). The injection of PRP-releasate significantly increased the number of chondrocyte-like cells in the NP compared with that of the PBS group (P <0.01). Values are shown as mean ± standard error of the mean.

PPP- and PRP-releasate. Our results showed that the mean T2 value in the AF and NP region of the PRP group was not increased significantly over other groups, even though a minor increase was seen. Additional samples may be needed to show treatment effects on T2 values, which may have been subtle.

The histological analyses showed that the injection of PRP-releasate induced an increase in the number of chondrocyte-like cells in the NP and the anterior inner AF, and this suggests tissue phenotype changes from fibrotic tissue to cartilaginous tissue. No inflammatory reactions, such as invasion of inflammatory cells or microvessels (or both), or ossification within the IVD tissue was found, suggesting that PRP-releasate had no adverse effects on disc tissues.

In the radiographic and histological analyses, PPP-releasate also induced a reparative effect on degenerated IVDs, although its effect was less than those of the PRP-releasate. Previous *in vitro* studies [21,22] have shown that PPP has effects on cell proliferation and matrix metabolism similar to those of fetal bovine serum, which is the most widely used serum supplement for *in vitro* cell culture; this suggests that PPP also contains growth factors and has the potential to stimulate the matrix metabolism of degenerated IVDs.

In the past, two different groups have performed *in vivo* intradiscal injection studies by using PRP to evaluate its effect on disc degeneration in animal models. Chen and colleagues [8] reported the effect of PRP on disc degeneration both in an *ex vivo* organ culture system and an *in vivo* porcine disc degeneration model. The releasate isolated from clotted PRP, which was induced by addition of bovine thrombin, was injected into the degenerated disc induced by chymopapain. In their study, PRP, which was shown to promote NP regeneration, also resulted in the upregulation of chondrogenesis and extracellular matrix accumulation. In the *in vivo* model, the recovery of disc height was not significant (P = 0.5). This may be due to the use of thrombin. With consideration for a future clinical application, we have decided not to use thrombin, but rather autologous serum and calcium, to activate PRP.

The other group [37,38] reported *in vivo* intradiscal injection studies using PRP-impregnated biodegradable gelatin hydrogel microspheres (PRP-GHMs) in a rabbit disc degeneration model induced by the partial aspiration of the NP with a 21-gauge needle. Two weeks after the initial surgery, autologous PRP alone or PRP-GHMs were injected into the degenerated discs. Contrary to the results of our study, the progression of disc degeneration was significantly suppressed by the combined administration of PRP-GHMs but not by PRP alone. Possible explanations for the conflicting findings concerning the effect of PRP would be, first, the differing methods used in the processing the injectable agents. We injected PRP-releasate isolated from activated platelets into the degenerated disc, whereas in the study by Nagae and colleagues [37], the PRP alone injected into the degenerated disc was prepared without platelet activation (without coagulation). Indeed, in an article just published, DeLong and colleagues [39] state that the manner in which platelet activation occurs is a variable

that determines the efficacy of PRP; they propose a classification system for PRP publications that includes 'platelet activation manner'. Second, differences in the disc degeneration animal models and evaluation methods could be reflected in the conflicting results. The anular puncture model has been shown to induce controlled and progressive disc degeneration and effectively detect the therapeutic effects [11,24,40]. A controlled degree of disc degeneration may be required to test the effects of biological therapies.

A limitation of this study is that the well-characterized rabbit anular puncture model [23] used is a short-term (1-month) injury animal model of disc degeneration. Although this model does not truly reflect the course of human disc degeneration, similar histological and biomechanical changes have been previously reported [11,23,24] and confirmed in this study. Therefore, the results of this study may contribute to the understanding of the cellular responses and the mechanism of the repair process after PRP application in degenerative discs.

Conclusions

We have shown that the administration of autologous PRP-releasate was effective in restoring disc height and increasing chondrocytic cells in the IVD of the rabbit anular puncture disc degeneration model. Importantly, the PRP-releasate prepared in this study was isolated from autologous PRP, which was activated without using xenogeneic or allogeneic blood products. The results of this study showing that the application of autologous PRP-releasate is effective for IVD therapy could provide valuable information for the consideration of PRP for a clinical application.

Abbreviations

AF: anulus fibrosus; ANOVA: analysis of variance; BMP: bone morphogenetic protein; DHI: disc height index; EGF: epidermal growth factor; GDF-5: growth differentiation factor-5; IGF-1: insulin-like growth factor-1; IL: interleukin; IVD: intervertebral disc; MRI: magnetic resonance imaging; NP: nucleus pulposus; OP-1: osteogenic protein-1; PBS: phosphate-buffered saline; PDGF: platelet-derived growth factor; PPP: platelet-poor plasma; PRP: platelet-rich plasma; PRP-GHM: platelet-rich plasma-impregnated biodegradable gelatin hydrogel microsphere; ROI: region of interest; TE: time-to-echo; TGF-β: transforming growth factor-β.

Acknowledgements

The authors thank Mary Ellen Lenz for her assistance in the preparation of the manuscript and acknowledge Takahiro Iino for his assistance in the preparation of tissue specimens. This study was supported by grants from the Ministry of Education, Culture, Sports, Science and Technology (Japan).

Author details

[1]Department of Orthopaedic Surgery, Mie University Graduate School of Medicine, 2-174 Edobashi, Tsu, 514-8507, Japan. [2]Department of Orthopaedic Surgery, University of California, San Diego, 9500 Gilman Drive, La Jolla, CA 92093-0863, USA. [3]Department of Radiology, University of California, San Diego, 408 Dickinson Street, San Diego, CA 92103-8226, USA. [4]Department of Spinal Surgery and Medical Engineering, Mie University Graduate School of Medicine, 2-174 Edobashi, Tsu, 514-8507, Japan.

Authors' contributions

SO helped to perform data acquisition and statistical analysis and write the manuscript. KA helped to perform data acquisition and statistical analysis and write the manuscript, conceived of this study, and made substantial contributions to the study design. KM contributed to the study design, interpreted the data, and finalized the manuscript. WB performed MRI data acquisition and interpreted the data. TI, RM, YA, and YK performed data acquisition. AU and AS contributed to the study design and coordination. All authors read and approved the final manuscript.

Competing interests

The authors declare that they have no competing interests.

Received: 26 July 2012 Revised: 13 October 2012
Accepted: 2 November 2012 Published: 5 November 2012

References

1. Kirkaldy-Willis WH, Wedge JH, Yong-Hing K, Reilly J: **Pathology and pathogenesis of lumbar spondylosis and stenosis.** *Spine (Phila Pa 1976)* 1978, **3**:319-328.
2. Osti OL, Fraser RD: **MRI and discography of annular tears and intervertebral disc degeneration. A prospective clinical comparison.** *J Bone Joint Surg Br* 1992, **74**:431-435.
3. Osti OL, Vernon-Roberts B, Moore R, Fraser RD: **Annular tears and disc degeneration in the lumbar spine. A post-mortem study of 135 discs.** *J Bone Joint Surg Br* 1992, **74**:678-682.
4. Videman T, Nurminen M: **The occurrence of anular tears and their relation to lifetime back pain history: a cadaveric study using barium sulfate discography.** *Spine (Phila Pa 1976)* 2004, **29**:2668-2676.
5. Lotz JC, Haughton V, Boden SD, An HS, Kang JD, Masuda K, Freemont A, Berven S, Sengupta DK, Tanenbaum L, Maurer P, Ranganathan A, Alavi A, Marinelli NL: **New treatments and imaging strategies in degenerative disease of the intervertebral disks.** *Radiology* 2012, **264**:6-19.
6. An HS, Takegami K, Kamada H, Nguyen CM, Thonar EJ, Singh K, Andersson GB, Masuda K: **Intradiscal administration of osteogenic protein-1 increases intervertebral disc height and proteoglycan content in the nucleus pulposus in normal adolescent rabbits.** *Spine (Phila Pa 1976)* 2005, **30**:25-31, discussion 31-22.
7. An HS, Thonar EJ, Masuda K: **Biological repair of intervertebral disc.** *Spine (Phila Pa 1976)* 2003, **28**:S86-92.
8. Chen WH, Liu HY, Lo WC, Wu SC, Chi CH, Chang HY, Hsiao SH, Wu CH, Chiu WT, Chen BJ, Deng WP: **Intervertebral disc regeneration in an ex vivo culture system using mesenchymal stem cells and platelet-rich plasma.** *Biomaterials* 2009, **30**:5523-5533.
9. Hiyama A, Mochida J, Iwashina T, Omi H, Watanabe T, Serigano K, Tamura F, Sakai D: **Transplantation of mesenchymal stem cells in a canine disc degeneration model.** *J Orthop Res* 2008, **26**:589-600.
10. Iwashina T, Mochida J, Sakai D, Yamamoto Y, Miyazaki T, Ando K, Hotta T: **Feasibility of using a human nucleus pulposus cell line as a cell source in cell transplantation therapy for intervertebral disc degeneration.** *Spine (Phila Pa 1976)* 2006, **31**:1177-1186.
11. Masuda K, Imai Y, Okuma M, Muehleman C, Nakagawa K, Akeda K, Thonar E, Andersson G, An HS: **Osteogenic protein-1 injection into a degenerated disc induces the restoration of disc height and structural changes in the rabbit anular puncture model.** *Spine (Phila Pa 1976)* 2006, **31**:742-754.
12. Nishida K, Kang JD, Gilbertson LG, Moon SH, Suh JK, Vogt MT, Robbins PD, Evans CH: **Modulation of the biologic activity of the rabbit intervertebral disc by gene therapy: an *in vivo* study of adenovirus-mediated transfer of the human transforming growth factor beta 1 encoding gene.** *Spine (Phila Pa 1976)* 1999, **24**:2419-2425.
13. Nishida K, Kang JD, Suh JK, Robbins PD, Evans CH, Gilbertson LG: **Adenovirus-mediated gene transfer to nucleus pulposus cells. Implications for the treatment of intervertebral disc degeneration.** *Spine (Phila Pa 1976)* 1998, **23**:2437-2442, discussion 2443.
14. Sakai D, Mochida J, Iwashina T, Watanabe T, Nakai T, Ando K, Hotta T: **Differentiation of mesenchymal stem cells transplanted to a rabbit**

degenerative disc model: potential and limitations for stem cell therapy in disc regeneration. *Spine (Phila Pa 1976)* 2005, 30:2379-2387.
15. Bae WC, Masuda K: **Emerging technologies for molecular therapy for intervertebral disk degeneration.** *Orthop Clin North Am* 2011, 42:585-601.
16. Alsousou J, Ali A, Willett K, Harrison P: **The role of platelet-rich plasma in tissue regeneration.** *Platelets* 2012, May 30. [Epub ahead of print].
17. Anitua E, Andia I, Ardanza B, Nurden P, Nurden AT: **Autologous platelets as a source of proteins for healing and tissue regeneration.** *Thromb Haemost* 2004, 91:4-15.
18. Reed G: **Platlet secretion.** *Platelets* London: Elsevier Science; 2002, 181-213.
19. Alsousou J, Thompson M, Hulley P, Noble A, Willett K: **The biology of platelet-rich plasma and its application in trauma and orthopaedic surgery: a review of the literature.** *J Bone Joint Surg Br* 2009, 91:987-996.
20. Man D, Plosker H, Winland-Brown JE: **The use of autologous platelet-rich plasma (platelet gel) and autologous platelet-poor plasma (fibrin glue) in cosmetic surgery.** *Plast Reconstr Surg* 2001, 107:229-237, discussion 238-229.
21. Akeda K, An HS, Okuma M, Attawia M, Miyamoto K, Thonar EJ, Lenz ME, Sah RL, Masuda K: **Platelet-rich plasma stimulates porcine articular chondrocyte proliferation and matrix biosynthesis.** *Osteoarthritis Cartilage* 2006, 14:1272-1280.
22. Akeda K, An HS, Pichika R, Attawia M, Thonar EJ, Lenz ME, Uchida A, Masuda K: **Platelet-rich plasma (PRP) stimulates the extracellular matrix metabolism of porcine nucleus pulposus and annulus fibrosus cells cultured in alginate beads.** *Spine (Phila Pa 1976)* 2006, 31:959-966.
23. Masuda K, Aota Y, Muehleman C, Imai Y, Okuma M, Thonar EJ, Andersson GB, An HS: **A novel rabbit model of mild, reproducible disc degeneration by an anulus needle puncture: correlation between the degree of disc injury and radiological and histological appearances of disc degeneration.** *Spine* 2005, 30:5-14.
24. Chujo T, An HS, Akeda K, Miyamoto K, Muehleman C, Attawia M, Andersson G, Masuda K: **Effects of growth differentiation factor-5 on the intervertebral disc–*in vitro* bovine study and *in vivo* rabbit disc degeneration model study.** *Spine (Phila Pa 1976)* 2006, 31:2909-2917.
25. Fallouh L, Nakagawa K, Sasho T, Arai M, Kitahara S, Wada Y, Moriya H, Takahashi K: **Effects of autologous platelet-rich plasma on cell viability and collagen synthesis in injured human anterior cruciate ligament.** *J Bone Joint Surg Am* 2010, 92:2909-2916.
26. Han B, Woodell-May J, Ponticiello M, Yang Z, Nimni M: **The effect of thrombin activation of platelet-rich plasma on demineralized bone matrix osteoinductivity.** *J Bone Joint Surg Am* 2009, 91:1459-1470.
27. Oprea WE, Karp JM, Hosseini MM, Davies JE: **Effect of platelet releasate on bone cell migration and recruitment *in vitro*.** *J Craniofac Surg* 2003, 14:292-300.
28. Tomoyasu A, Higashio K, Kanomata K, Goto M, Kodaira K, Serizawa H, Suda T, Nakamura A, Nojima J, Fukuda T, Katagiri T: **Platelet-rich plasma stimulates osteoblastic differentiation in the presence of BMPs.** *Biochem Biophys Res Commun* 2007, 361:62-67.
29. Furmaniak-Kazmierczak E, Cooke TD, Manuel R, Scudamore A, Hoogendorn H, Giles AR, Nesheim M: **Studies of thrombin-induced proteoglycan release in the degradation of human and bovine cartilage.** *J Clin Invest* 1994, 94:472-480.
30. Backes BJ, Harris JL, Leonetti F, Craik CS, Ellman JA: **Synthesis of positional-scanning libraries of fluorogenic peptide substrates to define the extended substrate specificity of plasmin and thrombin.** *Nat Biotechnol* 2000, 18:187-193.
31. Hascall VC, Sandy JD, Handley CJ: **Regulation of proteoglycan metabolism in articular cartilage.** *Biology of the Synovial Joint* Amsterdam, The Netherlands: OPA (Overseas Publishers Association) N.V.; 1999, 101-120.
32. Carragee EJ, Hurwitz EL, Weiner BK: **A critical review of recombinant human bone morphogenetic protein-2 trials in spinal surgery: emerging safety concerns and lessons learned.** *Spine J* 2011, 11:471-491.
33. Perry J, Haughton V, Anderson PA, Wu Y, Fine J, Mistretta C: **The value of T2 relaxation times to characterize lumbar intervertebral disks: preliminary results.** *AJNR Am J Neuroradiol* 2006, 27:337-342.
34. Trattnig S, Stelzeneder D, Goed S, Reissegger M, Mamisch TC, Paternostro-Sluga T, Weber M, Szomolanyi P, Welsch GH: **Lumbar intervertebral disc abnormalities: comparison of quantitative T2 mapping with conventional MR at 3.0 T.** *Eur Radiol* 2010, 20:2715-2722.
35. Watanabe A, Benneker LM, Boesch C, Watanabe T, Obata T, Anderson SE: **Classification of intervertebral disk degeneration with axial T2 mapping.** *AJR Am J Roentgenol* 2007, 189:936-942.
36. Welsch GH, Trattnig S, Paternostro-Sluga T, Bohndorf K, Goed S, Stelzeneder D, Mamisch TC: **Parametric T2 and T2* mapping techniques to visualize intervertebral disc degeneration in patients with low back pain: initial results on the clinical use of 3.0 Tesla MRI.** *Skeletal Radiol* 2011, 40:543-551.
37. Nagae M, Ikeda T, Mikami Y, Hase H, Ozawa H, Matsuda K, Sakamoto H, Tabata Y, Kawata M, Kubo T: **Intervertebral disc regeneration using platelet-rich plasma and biodegradable gelatin hydrogel microspheres.** *Tissue Eng* 2007, 13:147-158.
38. Sawamura K, Ikeda T, Nagae M, Okamoto S, Mikami Y, Hase H, Ikoma K, Yamada T, Sakamoto H, Matsuda K, Tabata Y, Kawata M, Kubo T: **Characterization of *in vivo* effects of platelet-rich plasma and biodegradable gelatin hydrogel microspheres on degenerated intervertebral discs.** *Tissue Eng Part A* 2009, 15:3719-3727.
39. Delong JM, Russell RP, Mazzocca AD: **Platelet-rich plasma: the PAW classification system.** *Arthroscopy* 2012, 28:998-1009.
40. Mwale F, Masuda K, Pichika R, Epure LM, Yoshikawa T, Hemmad A, Roughley PJ, Antoniou J: **The efficacy of Link N as a mediator of repair in a rabbit model of intervertebral disc degeneration.** *Arthritis Res Ther* 2011, 13:R120.

doi:10.1186/ar4084
Cite this article as: Obata *et al.*: Effect of autologous platelet-rich plasma-releasate on intervertebral disc degeneration in the rabbit anular puncture model: a preclinical study. *Arthritis Research & Therapy* 2012 14:R241.

THE JOURNAL OF GENE MEDICINE
J Gene Med 2012; **14**: 623–631.
Published online in Wiley Online Library (wileyonlinelibrary.com) **DOI:** 10.1002/jgm.2677

RESEARCH ARTICLE

Transfection of nuclear factor-kappaB decoy oligodeoxynucleotide protects against ischemia/reperfusion injury in a rat epigastric flap model

Takeshi Uemura
Masaya Tsujii*
Koji Akeda
Takahiro Iino
Haruhiko Satonaka
Masahiro Hasegawa
Akihiro Sudo

Department of Orthopaedic Surgery, Mie University Graduate School of Medicine, Tsu City, Japan

*Correspondence to: M. Tsujii, Department of Orthopaedic Surgery, Mie University Graduate School of Medicine, 2-174 Edobashi, Tsu City, Mie Prefecture 514-8507, Japan.
E-mail: m-t727@clin medic mie-uacjp

Received: 19 August 2012
Revised: 15 October 2012
Accepted: 16 October 2012

Abstract

Background Nuclear factor-kappaB (NF-κB) is considered to play an important role in the response to ischemia/reperfusion (I/R) injury in flap surgery. To inhibit NF-κB, synthetic double-stranded oligodeoxynucleotide (ODN) was used as a decoy. The present study aimed to evaluate the suppressive effects of NF-κB against I/R injury of experimental rat flap model.

Methods An extended epigastric island flap was raised and ischemia was induced for 3 h. NF-κB decoy ODN (group D) or single-strand ODN (control; group S) was injected via the contralateral artery when the pedicle was clamped. Transfection efficiency was evaluated with fluorescein isothiocyanate (FITC)-labeled ODN. The effects of NF-κB decoy ODN were analyzed in groups D and S, and an untreated group (group N).

Results FITC-labeled ODN was distributed over the entire flap. Mean survival rate of the flap was significantly higher in group D than in the other groups (group D: 57.9%; group S: 31.1%; group N 31.7%; $p < 0.005$). Injured muscle fibers, neutrophils and the expression of inducible nitric oxide synthase were significantly lower in group D. A real-time polymerase chain reaction also demonstrated a tendency for suppression of tumor necrosis factor-α, interleukin (IL)-1β and IL-6.

Conclusions We show that NF-κB decoy ODN protected against flap necrosis as a result of I/R injury in rats. We also indicate that intra-arterial injection of naked NF-κB decoy ODN is effective for transfection into target organs. Therefore, transfection of NF-κB decoy ODN represents a novel therapeutic strategy for the treatment of flap surgery in I/R injury. Copyright © 2012 John Wiley & Sons, Ltd.

Keywords flap necrosis; ischemia reperfusion injury; nuclear factor-kappaB; synthetic double-stranded oligodeoxynucleotide

Introduction

Tissue ischemia is a serious complication in numerous surgical specialties. Although the development of surgical techniques at tissue transfer has enabled the preservation of affected limb function as a result of severe trauma or malignant musculoskeletal tumor, the failure of reconstructive surgeries as a result of ischemia can lead to more extensive surgical revisions or limb amputation. One of the major problems in flap surgery is ischemia reperfusion (I/R) injury, in which the accumulation of inflammatory mediators and the production of reactive oxygen species plays a crucial role [1–4]. There have been numerous

reports of up-regulation of tumor necrosis factor (TNF)-α, interleukin (IL)-1, IL-6, intercellular adhesion molecule-1, monocyte chemoattractant protein-1 and inducible nitric oxide synthase (iNOS) in I/R injury [5–9]. Therefore, necrotic enhancement is expected to be overcome by inhibition of inflammatory processes, thus suggesting that blockage of inflammatory cascades improves outcomes in tissue transfer procedures such as skin flaps or transplantation of musculoskeletal organs.

One of the common signal pathways for these inflammatory factors is the nuclear transcription kappaB (NF-κB) pathway, which plays an important role in the regulation of immune and inflammatory systems in response to hypoxia, ischemia and I/R injury [10,11]. In the cell, NF-κB exists in an inactive state as a result of the binding of inhibitory protein IκB. When I/R injury is induced, IκB is phosphorylated, which results in the degradation of IκB. The free NF-κB moves to the nucleus from the cytoplasm, where it transactivates several target genes, such as those for TNF-α, IL-1, IL-6 and iNOS. Previous studies have indicated that skeletal muscle shows increased activation of NF-κB following I/R injury, and that inhibition of NF-κB activity decreases cytokines and increases muscle flap viability [10,12,13]. Wu *et al.* [14] reported that the administration of pyrrolidine dithiocarbamate, an NF-κB inhibitor, can improve flap survival in I/R injury in a rat skin flap model. Taken together, these results indicate that NF-κB is a key regulator of inflammatory molecules at the transcriptional level in ischemic tissues, thus suggesting that the inhibition of NF-κB is an ideal treatment against the progression of necrosis.

Various molecular biological methods to regulate the transcription of targeted genes have recently been developed and these are considered to represent a new antigene approach. To inhibit NF-κB activation, synthetic double-stranded oligodeoxynucleotide (ODN) as a 'decoy' *cis*-element against NF-κB has been introduced as a new strategy [15]. This reduces promoter activity by inhibiting the binding of the transcriptional regulator, and the mechanism is very simple compared to antisense DNA. NF-κB decoy ODN corresponding to *cis* sequences bind to activated NF-κB and suppress numerous inflammatory genes. Morishita *et al.* [16] reported the first successful transfer of NF-κB decoy ODN *in vivo* using this technology, and reduced the extent of myocardial infarction after reperfusion. Subsequently, the NF-κB decoy ODN strategy was reported as having therapeutic potential in various diseases, such as pulmonary metastasis by murine osteosarcoma [17], acute renal failure in rats [6], liver grafts in rats [7], rheumatoid arthritis in human synovial cells [18] and ultraviolet-induced cutaneous inflammation in mice [19]. However, it is difficult to achieve treatment effects, even when naked NF-κB decoy ODN is injected, because its entry into target cells is insufficient; 10 min after intravenous injection of naked NF-κB decoy, it is rapidly excreted in the urine [20].

A number of studies to improve flap survival have been performed, although there have been no reports on NF-κB inhibition at the gene level. The aims of the present study were: (i) to confirm whether intra-arterial application under pressure enhances the transfection efficiency of naked NF-κB decoy ODN; (ii) to evaluate the therapeutic effects of NF-κB decoy ODN against flap necrosis; and (iii) to histologically and biochemically analyze whether NF-κB decoy ODN inhibits inflammation and oxidative stress.

Materials and methods

Experimental animals

Thirty-nine male Sprague–Dawley rats weighing between 350 and 400 g (SLC, Hamamatsu, Japan) were used. All procedures were performed in accordance with protocols approved by the animal research committee of Mie University. Animals were individually maintained in the animal center of Mie University under a 12:12 h light/dark cycle with *ad libitum* access to food and water.

Surgical procedure

All rats were anesthetized with an intramuscular injection of a combination of ketamine 50 mg/kg and xylazine 2.5 mg/kg, the abdomen and groin were shaved, and the animal was placed in a supine position. An extended epigastric island flap, measuring 10 × 6 cm, was used as an experimental model [21]. The flap was raised from the left superficial epigastric artery and vein. A microvascular clamp was placed on the pedicle during the ischemic period. After flap elevation and induction of ischemia, each flap was sutured back to its original location. Thereafter, ischemia was induced for 3 h by clamping nutrient vessels. Of the 39 rats, 36 were used to study flap survival by histological and biochemical tests. The other three rats were used for the study of transfection efficiency.

Drug was slowly administrated over 5 min through the contralateral femoral artery (right femoral artery) using a 29-gauge dull needle when the pedicle was clamped. To administer the drug to the flap directly through the right superficial epigastric artery into the right femoral artery, the right femoral artery was dissected at the proximal point of the right superficial epigastric artery and vein bifurcation. The right femoral vein was ligated at the proximal and distal points of the right superficial epigastric artery and vein bifurcation.

Experimental design

Three different groups of 12 animals were established: group D, injection of NF-κB decoy ODN (5 mg/ml, 0.39 mM, 200 μl); group S, injection of single-strand ODN (10 mg/ml, 0.78 mM, 200 μl); and group N, no injection. The sequences of the phosphorothioate ODN used in the present study were: NF-κB decoy ODN, 5′-CCTTGAAGGGATTTCCCTCC-3′ and 3′-GGAACTTCCCTAAAGGGAGG-5′, and single-strand ODN, 5′-CCTTGAAGGGATTTCCCTCC-3′. Single-stranded

ODN was used as NF-κB decoy ODN control. NF-κB decoy ODN and single-stranded ODN were provided by AnGes MG (Osaka, Japan).

Transfection efficiency

To study the *in vivo* transfection efficiency of NF-κB decoy ODN, we used fluorescein isothiocyanate (FITC)-labeled decoy ODN. FITC-labeled phosphorothioate ODN labeled on the 3′- and 5′-ends of NF-κB decoy ODN was provided by AnGes MG. Transfection procedures were as described above. Flaps were harvested from four points (left and right half of the pedicle side of the flap, left and right half of the distal side of the flap) at 24 h after reperfusion ($n = 3$), and were fixed in 4% paraformaldehyde. Sections were examined by fluorescent microscopy. Nuclei were counterstained with propidium iodide (Invitrogen, Carlsbad, CA, USA).

Measurement of survival area of flap tissue

Survival area of the flap was evaluated at 5 days postoperatively ($n = 8$ for each). Zones of dark color were defined as necrotic, and the remaining areas were defined as viable. Flaps were stored as digital images, and survival area was calculated by image analysis software (Lumina Vision, version 1.11; Minami Shoji Co., Fukui, Japan). Survival rates were expressed as a percentage of the total flap area (survival rate = viable area/total area × 100%) [22].

Histopathological examination

Four animals in each group were used for histological study. Full-thickness 8-mm punch biopsy specimens were taken from one-third of the pedicle side after 24 h of reperfusion. Samples were immediately fixed in 4% paraformaldehyde for 24 h at 4 °C overnight, and were embedded in paraffin. Sections were cut at 5-μm thickness, placed on Silane-coated glass-slides (Matsunami, Osaka, Japan) and stained with hematoxylin and eosin to determine the infiltration of polymorphonuclear leukocytes (PMNs) in subcutaneous tissue and the panniculus carnosus muscle injury. Quantification of injured muscle fibers in the panniculus carnosus muscle was performed under microscopy at × 200 magnification in three sections for each slide. Injury scores were expressed as a percentage, as described previously [23]. The number of PMNs was evaluated at × 400 magnification in six sections for each slide [22].

RNA extraction and cDNA synthesis for quantitative real-time polymerase chain reaction (PCR)

We evaluated the production of TNF-α, IL-1β and IL-6 as inflammatory mediators. Full-thickness 8-mm punch biopsy specimens were taken from one-third of the pedicle side after 24 h of reperfusion ($n = 4$ for each). Total RNA was isolated using PureLink™ RNA Mini kit (Life Technologies Corporation, Carlsbad, CA, USA) in accordance with the manufacturer's instructions. Complementary DNA (cDNA) synthesis was performed by oligo (dt) 15 priming from 1 μg of total RNA using a cDNA synthesis kit (Roche, Mannheim, Germany) in accordance with the manufacturer's instructions. To quantify expression levels of TNF-α, IL-1β and IL-6 and GAPDH genes, real-time PCR amplification was performed on the ABI PRISM 7000 Sequence Detection System (Applied Biosystems, Foster City, CA, USA). TaqMan PCR was performed using TaqMan Universal PCR Master Mix (Applied Biosystems). TaqMan gene expression assay primers were ordered for the detection of rat TNF-α (assay ID. Rn01525859_g1), rat IL-1β (assay ID. Rn00580432_m1), rat IL-6 (assay ID. Rn01410330_m1) and rat GAPDH (assay ID. Rn99999916_s1; Applied Biosystems). Thermal cycling conditions were 50 °C for 2 min, 95 °C for 10 min, 40 cycles of 95 °C for 15 s, and 60 °C for 1 min. GAPDH was used as an endogenous reference gene for normalization. Expression levels of each gene were divided by GAPDH expression levels.

Immunohistochemical analysis of iNOS expression

Sections (5 μm) were deparaffinized and incubated in methanol containing 0.3% H_2O_2 for 30 min to block intrinsic peroxidase activity. Sections were then treated with 0.01 M citrate buffer at 97 °C for 30 min to retrieve antigens, and were treated with primary antibodies and rabbit polyclonal anti-iNOS antibody (Thermo Fisher Scientific, Waltham, MA, USA) at room temperature overnight. After washing, sections were incubated with horseradish peroxidase-conjugated anti-rabbit immunoglobulin G Fab′ (dilution 1:100; DAKO, Glostrup, Denmark) at room temperature for 1 h, followed by catalysis for signal amplification (CSA II; DAKO). The morphometric evaluation method was as employed as described previously [24]. Color video images of three sections for each slide were captured randomly and digitized using a BX50 microscope (Olympus, Tokyo, Japan) connected to a computer. The percentage of iNOS-expression areas at the panniculus carnosus muscle on the digital images was calculated as the sum total of stained areas divided by the total area of the panniculus carnosus muscle using image analysis software (Lumina Vision, version 1.11).

Statistical analysis

StatView, version 5.0 (SAS Institute, Cary, NC, USA) was used for statistical analysis. Data are expressed as the mean ± SE and analyzed using Fisher's post-hoc least significant difference test. $p < 0.05$ was considered statistically significant.

Results

Intra-arterial injection of naked NF-κB decoy ODN was effectively transfected

At 24 h after reperfusion, FITC-labeled decoy ODN was distributed over the entire flap (Figure 1), thus suggesting that NF-κB decoy ODN was fully carried and maintained in the entire flap, including the distal end by application within the artery. Furthermore, FITC-labeled decoy ODN was not observed in the epidermal and corium layers but was present in the subcutaneous tissue, including adipose tissue and the panniculus carnosus muscle layer. It was particularly surprising that NF-κB decoy ODN was clearly observed in the nuclei of the panniculus carnosus muscle (Figure 2).

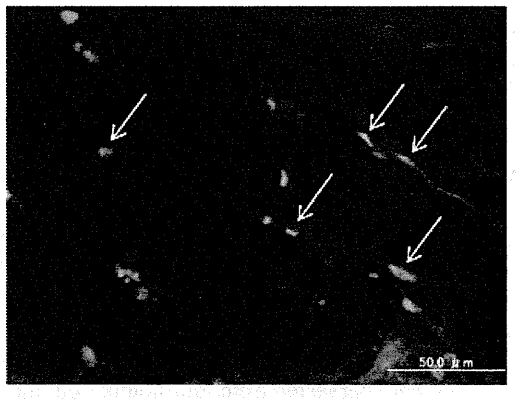

Figure 2. The section was observed under confocal microscopy to identify the localization of FITC-labeled decoy ODN. FITC-labeled decoy ODN was observed in the nuclei in muscle tissue (arrowheads). Nuclei were stained with propidium iodide (red).

NF-κB decoy ODN significantly suppressed I/R injury on microscopic and macroscopic findings

At postoperative day 5, the mean flap survival areas in groups D, S and N was 57.9 ± 8.4%, 31.1 ± 3.7% and 31.7 ± 4.8%, respectively (Figure 3). Group D showed a significant increase in viability compared to groups S and N (Figure 4). In addition, there were two subjects with complete flap survival in group D. With regard to subcutaneous tissue damage, we histologically evaluated the muscle fibers of the panniculus carnosus muscle in the macroscopically surviving area because muscles are easily affected by blood flow. In injured muscle fibers, values per field at 24 h were: group D, 21.0 ± 5.3% per field; group

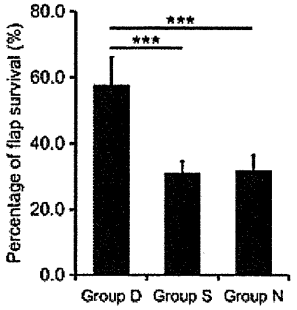

Figure 3. Survival rate of skin flaps after ischemia at 5 days postoperatively. When group D (57.9 ± 8.4%) was compared with the other groups (group S, 31.1 ± 3.7%; group N, 31.7 ± 4.8%), the increases in survival were statistically significant. Results were calculated from experiments with eight rats. Each value represents the mean ± SE. ***$p < 0.005$.

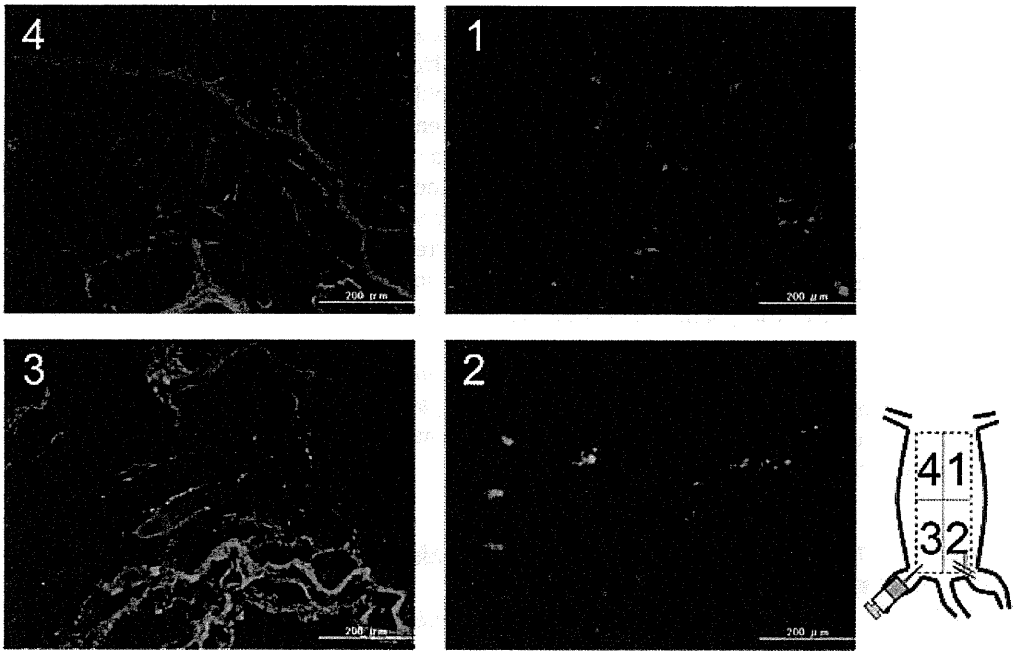

Figure 1. Representative microscopic findings of distribution of FITC-labeled decoy ODN. After 24 h of reperfusion, FITC-labeled decoy ODN was seen at four sites in the flap (green). An extended epigastric island flap, measuring 10 × 6 cm, was raised from the left superficial epigastric artery and vein. Flaps were divided into four segments of equal size (1, 2, 3 and 4).

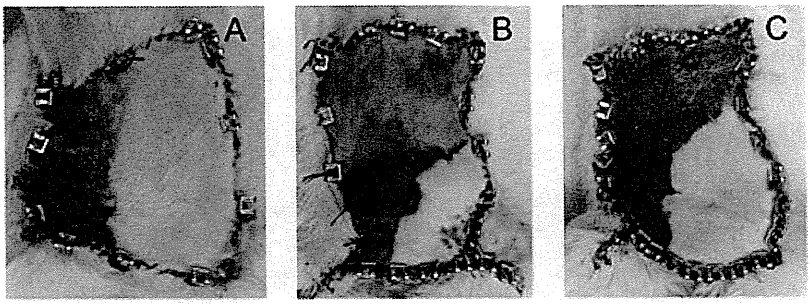

Figure 4. Digital photographs of the extended epigastric island skin flaps in group D (A), group S (B) and group N (C) at 5 days post-operatively. Clear demarcation of necrotic and viable regions is observed.

S, 46.4 ± 5.2% per field; and group N, 47.3 ± 7.1% per field, respectively. Mean injured muscle fibers in the NF-κB decoy ODN-transfected group were significantly lower compared to groups S and N (Figure 5). It appears that the NF-κB decoy ODN-transfected group maintained both the individual morphological changes of myocytes and the muscular bundle structure.

Inhibition of NF-κB protected flap tissues from inflammation and oxidative stress as a result of I/R injury

We evaluated PMNs accumulation and gene expression of TNF-α, IL-1β and IL-6 as marker of inflammation. Histopathological results for PMNs counts per field at 24 h were: group D, 7.0 ± 0.73 per field; group S, 14.0 ± 2.7 per field; and group N, 12.4 ± 1.7 per field. Group D showed a significant decrease in the accumulation of PMNs compared to groups S and N (Figure 6). There were no differences between group S and N. On real-time PCR, the transfection of NF-κB decoy ODN decreased the expression of TNF-α, IL-1β and IL-6 at the mRNA level compared to groups S and N, although there were no significant differences (Figure 7). With regard to oxidative stress, we performed immunohistochemical analysis of iNOS and morphometric analysis. In groups S and N, iNOS protein was clearly expressed in the panniculus carnosus muscle. By contrast, transfection of NF-κB decoy ODN decreased iNOS expression. The percentage of iNOS-expressing tissue in the panniculus carnosus muscle was: group D, 7.0 ± 1.2%; group S, 13.0 ± 1.2%; and group N, 13.4 ± 1.9%. NF-κB decoy ODN significantly suppressed iNOS expression in panniculus carnosus muscle (Figure 8).

Discussion

I/R injury has remained a significant problem in reconstructive surgery. When the blood supply is restored, various factors lead to additional cell damage beyond the primary

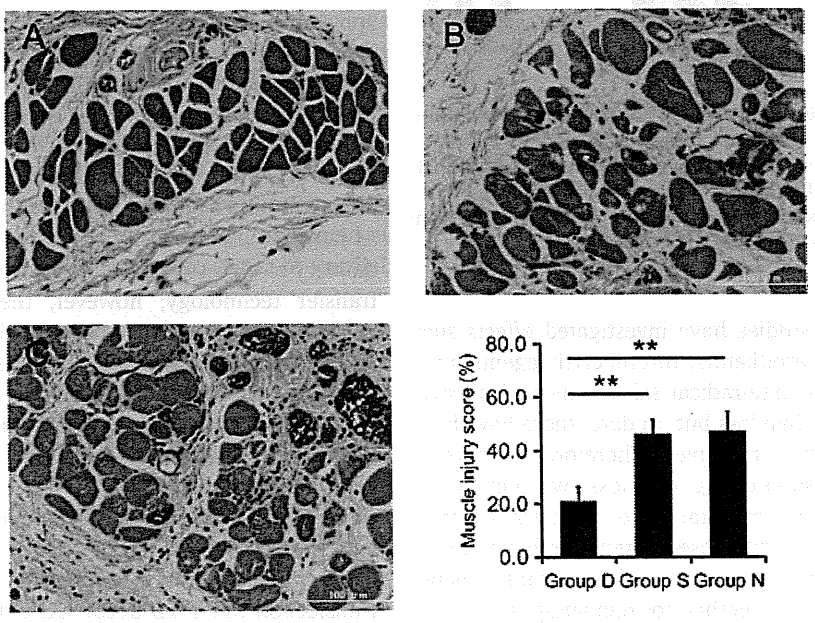

Figure 5. Representative photomicrographs of injured muscle fibers and injury scores (× 200 magnification). Histopathological results demonstrated that the group treated by NF-κB decoy ODN maintained myofiber morphology, whereas the mean numbers of injured muscle fibers in group D (21.0 ± 5.3%) were significantly lower than those in groups S (46.4 ± 5.2%) and N (47.3 ± 7.1%). (A) group D; (B) group S; (C) group N; Each value represents the mean ± SE. $^{**}p < 0.01$.

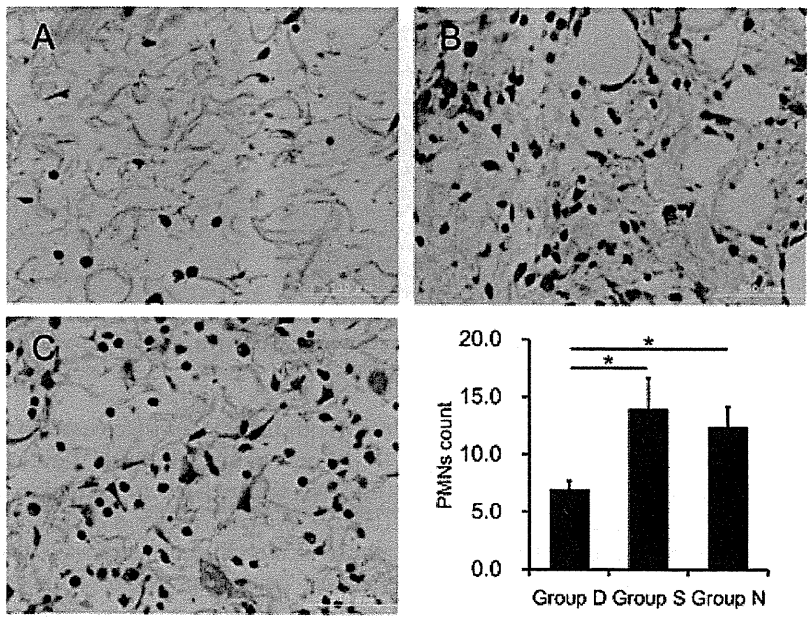

Figure 6. Representative photomicrographs of PMNs infiltration (× 400 magnification). PMN count at 24 h after reperfusion for groups D (7.0 ± 0.73 per field), S (14.0 ± 2.7 per field) and N (12.4 ± 1.7 per field). Each group consists of six animals. Treatment with NF-κB decoy ODN significantly decreased PMN accumulation relative to other groups. (A) group D; (B) group S; (C) group N; Each value represents the mean ± SE. *$p < 0.05$.

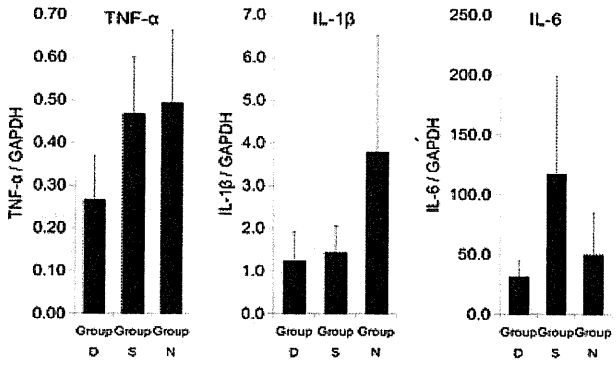

Figure 7. Effects of NF-κB decoy ODN transfection on expression of TNF-α, IL-1β and IL-6 in the flap after I/R injury *in vivo*. Expression levels of each gene were normalized against GAPDH expression levels. Although no significant differences were noted, some suppression of inflammatory mRNA expression was noted. Each value represents the mean ± SE.

ischemia. Previous studies have investigated effects such as anticoagulants, vasodilators, thrombolytic agents, anti-inflammatory drugs, free-radical scavengers and surgical procedures to avoid flap loss but, to date, there have been no established clinical therapies. Therefore, to develop new methods for suppressing flap loss, we focused on NF-κB, which plays an important role in the transcription of various genes, primarily those related to inflammation.

As genetic research has progressed, disease-causing genes have been clarified. As a method for regulating the appearance of target proteins, there are target molecule expression control strategies that use nucleic acid drugs, such as antisense DNA and small interfering RNA, including the decoy ODN technology used in this study. Bielinska *et al.* [25] introduced the notion that double-stranded phosphorothioate oligonucleotides compete for binding to their specific target sequences. Indeed, synthetic double-stranded ODN acting as a decoy *cis*-element effectively bound NF-κB to promoter regions and inhibited its activity, thereby blocking the transactivation of genes for essential cytokines *in vivo* in several animal models of inflammatory disease, as well as *in vitro* [16,26–29].

On the other hand, one of the obstacles to the therapeutic application of NF-κB decoy ODN is the lack of efficient delivery to target cells *in vivo*. Oligonucleotides are degraded by plasma deoxyribonuclease [30]. In animal models, intravenously injected naked NF-κB decoy was rapidly excreted in the urine and accumulated in the kidney, although there was little accumulation in other organs [20]. Previous studies proposed virus-mediated procedures, such as hemagglutinating virus of Japan (HVJ) liposomes, for delivery to target cells [31]. Viral vectors are a novel gene transfer technology; however, there remain numerous problems, such as immunosuppression and lethal toxicity, and these safety issues have not been resolved clinically. Therefore, a number of studies have been performed using gene transfer methods without viral vectors, including ultrasound-mediated gene transfer [32,33], ointment-containing NF-κB decoy ODN [34], intracolonic administration of NF-κB decoy ODN [35] and local delivery using NF-κB decoy ODN-eluting stents during expansion by balloon dilatation [36]. Yamasaki *et al.* [37] reported that transfection of NF-κB decoy ODN directly during balloon inflation suppressed neointimal formation in a porcine coronary artery model. These results suggested that the transfection efficiency of NF-κB decoy ODN could be increased by applying intravascular pressure during

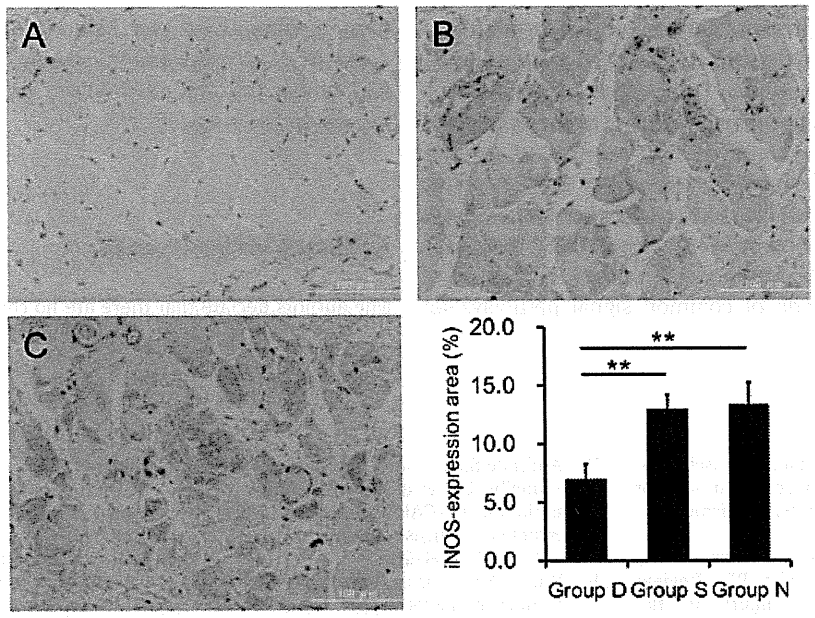

Figure 8. Representative photomicrographs of immunohistochemical staining of iNOS expression in the muscle after I/R injury. Muscle from rats in groups S and N revealed strong iNOS expression, although marked decreases in iNOS expression from group D were observed. Semi-quantitative analysis revealed that administration of NF-κB decoy ODN could down-regulate iNOS expression (group D, 7.0 ± 1.2%; group S, 13.0 ± 1.2%; group N, 13.4 ± 1.9%). (A) group D; (B) group S; (C) group N; Each value represents the mean ± SE. $^{**}p < 0.01$.

ischemia via an arterial clamp on the flap. Indeed, we showed that this method of application effectively enhances the transfection efficiency of naked NF-κB decoy ODN, in which NF-κB decoy ODN was delivered to the whole flap for 24 h after injection, and was shown to be transfected into nuclei. The method of intra-arterial injection is not technically difficult because surgeons familiar with microsurgical techniques have observed that the elevated flaps always include several nutrient vessels. We are convinced that it is possible to apply this administration method to viable clinical applications in humans.

To evaluate the therapeutic effects of NF-κB decoy ODN, the viability of flap survival was assessed by macroscopic findings on postoperative day 5. Group D showed a significant increase in viability compared to the other groups. As shown in the results obtained in the present study, the method for blocking the NF-κB pathway using NF-κB decoy ODN is expected as a new strategy for skin flap necrosis inhibition. On the other hand, there were no clear necrotic findings macroscopically at 24 h after elevating the flap of all groups; nevertheless, histological changes were observed in the control and untreated groups. Previous studies indicated that NF-κB is activated within 24 h after reperfusion [12,14], and attenuation of NF-κB activity early in the course of reperfusion may have protected against a severe I/R injury and inhibited flap necrosis. The causes of flap loss after I/R injury are multifactorial, and include PMNs, reactive oxygen species, cytokines, complement, mast cells and immune complexes [1,3]. Among these, we assessed inflammation changes and oxidative stress related to NF-κB in the early stages.

We examined PMNs infiltration, inflammation-related gene expression and iNOS expression for oxidative stress at 24 h after reperfusion. Previous studies have suggested that infiltration of inflammatory cells, such as PMNs, are crucial in I/R injury [38], whereas infiltration of PMNs into skeletal muscle [39], skin flaps [40] and myocardium [41] after I/R injury has been confirmed in animal models. In addition, a number of experimental studies have demonstrated improved flap survival rates by inhibiting neutrophil infiltration with lidocaine [42] or montelukast [22], and by inhibiting NF-κB activity [13,14]. In the present study, histopathological analysis showed a decrease in inflammatory cells with transfection of NF-κB decoy ODN. Furthermore, although there were no significant differences, the expression of TNF-α, IL-1β and IL-6 at the mRNA level decreased with transfection of NF-κB decoy ODN. iNOS expression was also decreased in the NF-κB decoy ODN-transfected group compared to the other groups in the present study. In particular, iNOS expression was significantly inhibited in the panniculus carnosus muscle, which was strongly transfected with NF-κB decoy ODN. In groups S and N, inflammatory changes and oxidative stress were not controlled, and muscle fibers were markedly damaged. Two NF-κB binding sites exist in the iNOS promoter [43], and a relationship has been reported between NF-κB and iNOS in I/R injury [10,44], thus suggesting that application of NF-κB decoy ODN is able to directly inhibit the expression of iNOS. Furthermore, the muscles exposed in I/R injury express or activate inflammatory cytokines, which stimulate the proliferation and migration of PMNs, and these PMNs can produce inflammatory cytokines. Blockade of this cascade by NF-κB decoy ODN may directly, as well as indirectly, prevent the development of progressive events leading to flap necrosis.

In conclusion, the present study shows that intra-arterial injection within raised flap arteries is effective for transfection into target organs *in vivo*. Transfection of NF-κB decoy ODN significantly protected muscle fibers in the panniculus carnosus muscle and improved flap survival in the I/R injury model. For the pathophysiology of improved flap survival, the present histological and biochemical analyses suggest that transfection of NF-κB decoy ODN decreased the infiltration of inflammatory cells and the expression of iNOS through blockade of common signal pathways for these inflammatory and oxidative factors. Thus, NF-κB decoy ODN provides a novel strategy for the prevention of flap failure following I/R injury and may be useful for reconstructive surgery.

Acknowledgements

The authors declare that there are no conflicts of interest.

References

1. Siemionow M, Arslan E. Ischemia/reperfusion injury: a review in relation to free tissue transfers. *Microsurgery* 2004; **24**: 468–475.
2. van den Heuvel MG, Buurman WA, Bast A, van der Hulst RR. Review: ischaemia-reperfusion injury in flap surgery. *J Plast Reconstr Aesthet Surg* 2009; **62**: 721–726.
3. Khalil AA, Aziz FA, Hall JC. Reperfusion injury. *Plast Reconstr Surg* 2006; **117**: 1024–1033.
4. Carroll WR, Esclamado RM. Ischemia/reperfusion injury in microvascular surgery. *Head Neck* 2000; **22**: 700–713.
5. Ozer K, Adanali G, Siemionow M. Late effects of TNF-alpha-induced inflammation on the microcirculation of cremaster muscle flaps under intravital microscopy. *J Reconstr Microsurg* 2002; **18**: 37–45.
6. Cao CC, Ding XQ, Ou ZL, *et al.* In vivo transfection of NF-kappaB decoy oligodeoxynucleotides attenuate renal ischemia/reperfusion injury in rats. *Kidney Int* 2004; **65**: 834–845.
7. Xu MQ, Shuai XR, Yan ML, Zhang MM, Yan LN. Nuclear factor-kappaB decoy oligodeoxynucleotides attenuates ischemia/reperfusion injury in rat liver graft. *World J Gastroenterol* 2005; **11**: 6960–6967.
8. Chandrasekar B, Streitman JE, Colston JT, Freeman GL. Inhibition of nuclear factor kappa B attenuates proinflammatory cytokine and inducible nitric-oxide synthase expression in postischemic myocardium. *Biochim Biophys Acta* 1998; **1406**: 91–106.
9. Zhang F, Hu EC, Topp S, Lei M, Chen W, Lineaweaver WC. Proinflammatory cytokines gene expression in skin flaps with arterial and venous ischemia in rats. *J Reconstr Microsurg* 2006; **22**: 641–647.
10. Park JW, Qi WN, Cai Y, Urbaniak JR, Chen LE. Proteasome inhibitor attenuates skeletal muscle reperfusion injury by blocking the pathway of nuclear factor-kappaB activation. *Plast Reconstr Surg* 2007; **120**: 1808–1818.
11. Latanich CA, Toledo-Pereyra LH. Searching for NF-kappaB-based treatments of ischemia reperfusion injury. *J Invest Surg* 2009; **22**: 301–315.
12. Lille ST, Lefler SR, Mowlavi A, *et al.* Inhibition of the initial wave of NF-kappaB activity in rat muscle reduces ischemia/reperfusion injury. *Muscle Nerve* 2001; **24**: 534–541.
13. Andrade-Silva AR, Ramalho FS, Ramalho LN, *et al.* Effect of NFkappaB inhibition by CAPE on skeletal muscle ischemia-reperfusion injury. *J Surg Res* 2009; **153**: 254–262.
14. Wu X, Yu M, Li A. Protective effect of a nuclear factor-kappaB inhibitor on ischemia-reperfusion injury in a rat epigastric flap model. *J Reconstr Microsurg* 2008; **24**: 351–359.
15. Morishita R, Tomita N, Kaneda Y, Ogihara T. Molecular therapy to inhibit NFkappaB activation by transcription factor decoy oligonucleotides. *Curr Opin Pharmacol* 2004; **4**: 139–146.
16. Morishita R, Sugimoto T, Aoki M, *et al.* In vivo transfection of cis element 'decoy' against nuclear factor-kappaB binding site prevents myocardial infarction. *Nat Med* 1997; **3**: 894–899.
17. Nishimura A, Akeda K, Matsubara T, *et al.* Transfection of NF-kappaB decoy oligodeoxynucleotide suppresses pulmonary metastasis by murine osteosarcoma. *Cancer Gene Ther* 2011; **18**: 250–259.
18. Tomita T, Takano H, Tomita N, *et al.* Transcription factor decoy for NFkappaB inhibits cytokine and adhesion molecule expressions in synovial cells derived from rheumatoid arthritis. *Rheumatology (Oxford)* 2000; **39**: 749–757.
19. Abeyama K, Eng W, Jester JV, *et al.* A role for NF-kappaB-dependent gene transactivation in sunburn. *J Clin Invest* 2000; **105**: 1751–1759.
20. Higuchi Y, Kawakami S, Oka M, Yabe Y, Yamashita F, Hashida M. Intravenous administration of mannosylated cationic liposome/NFkappaB decoy complexes effectively prevent LPS-induced cytokine production in a murine liver failure model. *FEBS Lett* 2006; **580**: 3706–3714.
21. Kuntscher MV, Schirmbeck EU, Menke H, Klar E, Gebhard MM, Germann G. Ischemic preconditioning by brief extremity ischemia before flap ischemia in a rat model. *Plast Reconstr Surg* 2002; **109**: 2398–2404.
22. Gideroglu K, Yilmaz F, Aksoy F, Bugdayci G, Saglam I, Yimaz F. Montelukast protects axial pattern rat skin flaps against ischemia/reperfusion injury. *J Surg Res* 2009; **157**: 181–186.
23. McCormack MC, Kwon E, Eberlin KR, *et al.* Development of reproducible histological injury severity scores: skeletal muscle reperfusion injury. *Surgery* 2008; **143**: 126–133.
24. Tsujii M, Hirata H, Yoshida T, Imanaka-Yoshida K, Morita A, Uchida A. Involvement of tenascin-C and PG-M/versican in flexor tenosynovial pathology of idiopathic carpal tunnel syndrome. *Histol Histopathol* 2006; **21**: 511–518.
25. Bielinska A, Shivdasani RA, Zhang LQ, Nabel GJ. Regulation of gene expression with double-stranded phosphorothioate oligonucleotides. *Science* 1990; **250**: 997–1000.
26. Sawa Y, Morishita R, Suzuki K, *et al.* A novel strategy for myocardial protection using *in vivo* transfection of cis element 'decoy' against NFkappaB binding site: evidence for a role of NFkappaB in ischemia-reperfusion injury. *Circulation* 1997; **96**: II-280–284; discussion II-285.
27. Tomita N, Morishita R, Tomita S, *et al.* Transcription factor decoy for NFkappaB inhibits TNF-alpha-induced cytokine and adhesion molecule expression *in vivo*. *Gene Ther* 2000; **7**: 1326–1332.
28. Tomita N, Morishita R, Lan HY, *et al.* In vivo administration of a nuclear transcription factor-kappaB decoy suppresses experimental crescentic glomerulonephritis. *J Am Soc Nephrol* 2000; **11**: 1244–1252.
29. Tomita N, Morishita R, Tomita S, *et al.* Inhibition of TNF-alpha, induced cytokine and adhesion molecule. Expression in glomerular cells *in vitro* and *in vivo* by transcription factor decoy for NFkappaB. *Exp Nephrol* 2001; **9**: 181–190.
30. Miyao T, Takakura Y, Akiyama T, Yoneda F, Sezaki H, Hashida M. Stability and pharmacokinetic characteristics of oligonucleotides modified at terminal linkages in mice. *Antisense Res Dev* 1995; **5**: 115–121.
31. Matsuda N, Hattori Y, Jesmin S, Gando S. Nuclear factor-kappaB decoy oligodeoxynucleotides prevent acute lung injury in mice with cecal ligation and puncture-induced sepsis. *Mol Pharmacol* 2005; **67**: 1018–1025.
32. Inagaki H, Suzuki J, Ogawa M, Taniyama Y, Morishita R, Isobe M. Ultrasound-microbubble-mediated NF-kappaB decoy transfection attenuates neointimal formation after arterial injury in mice. *J Vasc Res* 2006; **43**: 12–18.
33. Azuma H, Tomita N, Kaneda Y, *et al.* Transfection of NFkappaB-decoy oligodeoxynucleotides using efficient ultrasound-mediated gene transfer into donor kidneys prolonged survival of

rat renal allografts. *Gene Ther* 2003; **10**: 415–425.
34. Nakamura H, Aoki M, Tamai K, *et al.* Prevention and regression of atopic dermatitis by ointment containing NF-kB decoy oligodeoxynucleotides in NC/Nga atopic mouse model. *Gene Ther* 2002; **9**: 1221–1229.
35. De Vry CG, Prasad S, Komuves L, *et al.* Non-viral delivery of nuclear factor-kappaB decoy ameliorates murine inflammatory bowel disease and restores tissue homeostasis. *Gut* 2007; **56**: 524–533.
36. Ohtani K, Egashira K, Nakano K, *et al.* Stent-based local delivery of nuclear factor-kappaB decoy attenuates in-stent restenosis in hypercholesterolemic rabbits. *Circulation* 2006; **114**: 2773–2779.
37. Yamasaki K, Asai T, Shimizu M, *et al.* Inhibition of NFkappaB activation using cis-element 'decoy' of NFkappaB binding site reduces neointimal formation in porcine balloon-injured coronary artery model. *Gene Ther* 2003; **10**: 356–364.
38. Kirschner RE, Chiao JJ, Fyfe BS, Hoffman LA, Davis JM, Fantini GA. Neutrophil lipoxygenase activation and leukosequestration in postischemic myocutaneous flaps: role of LTB4. *Am J Physiol* 1995; **268**: H2167–2174.
39. Lee C, Kerrigan CL, Tellado JM. Altered neutrophil function following reperfusion of an ischemic myocutaneous flap. *Plast Reconstr Surg* 1992; **89**: 916–923.
40. Lee C, Kerrigan CL. Neutrophil localization following reperfusion of ischemic skin flaps. *Plast Reconstr Surg* 1992; **89**: 910–915.
41. Kin H, Wang NP, Halkos ME, Kerendi F, Guyton RA, Zhao ZQ. Neutrophil depletion reduces myocardial apoptosis and attenuates NFkappaB activation/TNFalpha release after ischemia and reperfusion. *J Surg Res* 2006; **135**: 170–178.
42. Eskitascioglu T, Karaci S, Canoz O, Kilic E, Gunay GK. The impact of lidocaine on flap survival following reperfusion injury. *J Surg Res* 2011; **167**: 323–328.
43. Xie QW, Kashiwabara Y, Nathan C. Role of transcription factor NF-kappa B/Rel in induction of nitric oxide synthase. *J Biol Chem* 1994; **269**: 4705–4708.
44. Qi WN, Chaiyakit P, Cai Y, *et al.* NF-kappaB p. 65 involves in reperfusion injury and iNOS gene regulation in skeletal muscle. *Microsurgery* 2004; **24**: 316–323.

J Orthop Sci
DOI 10.1007/s00776-012-0284-y

CASE REPORT

Arthroscopically assisted minimally invasive plate osteosynthesis for posterior fracture–dislocation of the shoulder

Aki Fukuda · Akinobu Nishimura · Ko Kato · Akihiro Sudo

Received: 21 April 2012 / Accepted: 26 July 2012

Introduction

Proximal humeral fractures are becoming increasingly common, and treatment of displaced proximal humeral fractures remains a challenge. Minimally invasive plate osteosynthesis (MIPO), which provides early functional recovery, is a promising treatment option for proximal humeral fractures [1]. We report a patient with posterior fracture–dislocation of the shoulder who was successfully treated with arthroscopic reduction and plate fixation via a minimally invasive approach.

Case report

A 35-year-old man fell down stairs and landed on his right shoulder and complained of severe pain. Physical examination revealed gross swelling and tenderness in his right shoulder. Motion was severely restricted due to pain; neurovascular examination was normal. Plain radiographs showed complex posterior fracture–dislocation (Fig. 1). Computed tomography (CT) showed intra-articular fracture involving both tuberosities in addition to anatomical neck fracture (Fig. 2). Arthroscopically assisted reduction was performed under general anesthesia, and findings showed a displaced humeral head fragment involving the articular surface (Fig. 3a). Posteriorly dislocated humeral head was reduced by gentle manipulation using a blunt trocar from the posterior portal and the joy-stick technique using a K wire. After reduction, stable articular surface reduction of the humeral head was obtained (Fig. 3b). The proximal humeral fracture was fixed using minimally invasive plate osteosynthesis (MIPO) (NCB plate, Zimmer, Warsaw, IN, USA) via the anterolateral acromial approach (Fig. 4). The patient began gentle active mobilization exercises after 2 weeks. Six months after the operation, the implant was removed. At follow-up 15 months after the operation, the shoulder was pain free, had 160° flexion, 40° external rotation, and internal rotation to the level of the eighth thoracic spine. The patient reported no limitation in daily activities and no evidence of nerve palsy; his Japanese Orthopaedic Association (JOA) score was 90 out of 100. Radiographs showed fracture union and no evidence of avascular necrosis of the humeral head (Fig. 5).

Each author certifies that his or her institution approved the human protocol for this investigation, that all investigations were conducted in conformity with ethical principles of research, and that informed consent was obtained.

Discussion

Posterior fracture–dislocation of the shoulder is an extremely rare injury, constituting 0.9 % [2] of proximal humeral fractures and occurring annually in 0.6/100,000 people [3]. The most common fracture associated with posterior dislocation of the shoulder is humeral head impression fracture. In addition, an associated fracture of the anatomical neck or tuberosities may be present. On the basis of the location of the fracture lines, the injury is classified into

A. Fukuda (✉) · A. Nishimura · K. Kato · A. Sudo
Department of Orthopaedic Surgery,
Mie University Faculty of Medicine,
2-174 Edobashi, Tsu, Mie 514-8507, Japan
e-mail: aki0611@clin.medic.mie-u.ac.jp

A. Fukuda
Department of Orthopaedic Surgery,
Suzuka Kaisei Hospital, Suzuka, Mie, Japan

Published online: 10 October 2012

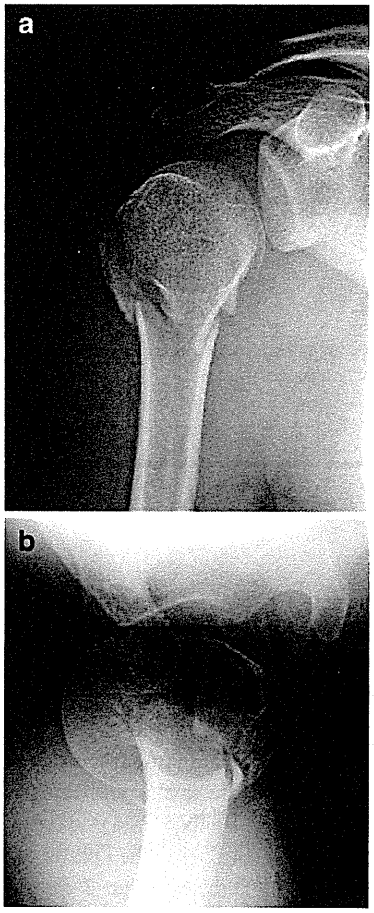

Fig. 1 Anteroposterior (**a**) and axillary (**b**) radiographs immediately after injury

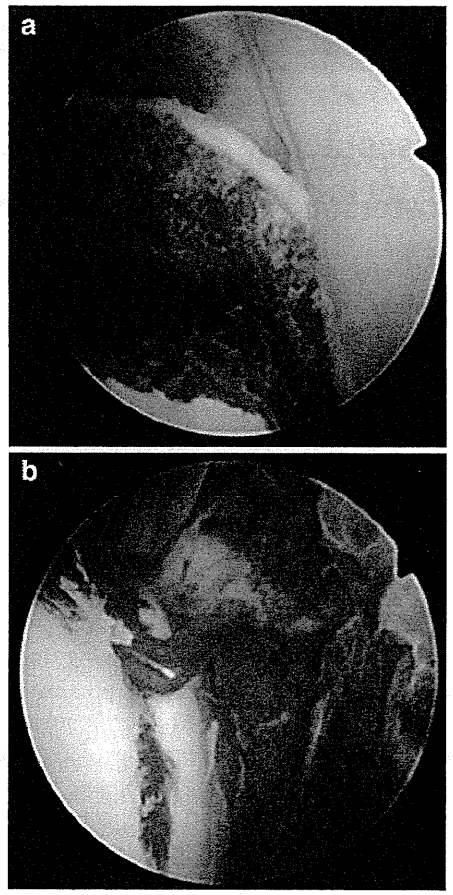

Fig. 3 Arthroscopic views from the anterior portal view show a displaced humeral head fragment (**a**) and complete reduction of the articular surface (**b**)

three types: type 1, Neer two-part anatomical neck fracture; type 2, Neer three-part fracture of the lesser tuberosities; type 3, Neer three-part fracture with composite tuberosity "shield" fragment [3]. The injury to our patient was classified as type 3 because it involved both tuberosities and an anatomical neck fracture.

Reduction should be performed gently under direct vision because closed reduction may lead to further

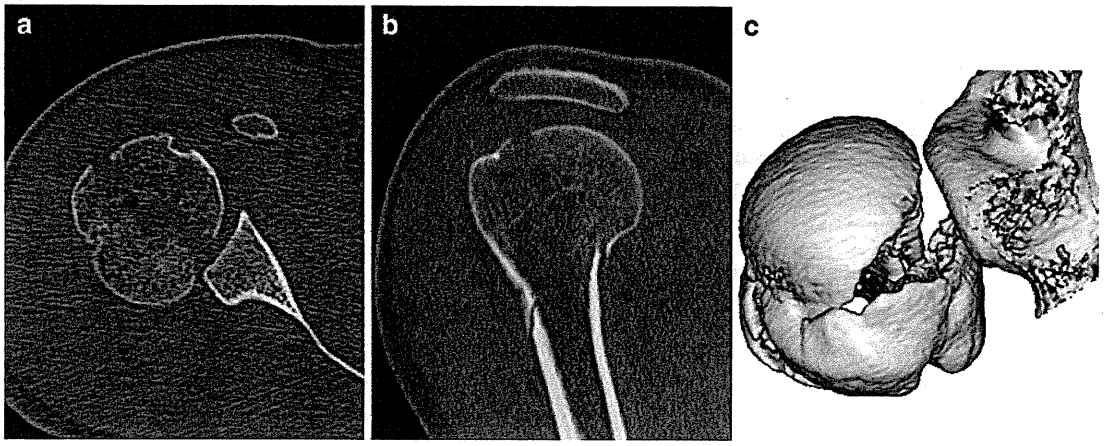

Fig. 2 Computed tomography (CT) scans in axial (**a**), coronal (**b**), and three-dimensional reconstruction (**c**) images immediately after injury

Fig. 4 Postoperative radiographs in the anteroposterior view after minimally invasive plate osteosynthesis (MIPO)

fracture displacement and result in avascular necrosis of the humeral head [4], the incidence of which after displaced proximal humeral fractures ranges from 21 % to 75 % [5–7]. Open reduction through anterior, deltoid-splitting, and posterior approaches was associated with poor visualization of the articular congruency and concomitant intra-articular pathology. Moreover, surgical exposure, such as the deltopectoral approach, may risk injury to blood vessels that are important to the proximal humerus. In our patient, the arthroscopic procedure enabled accurate anatomical reduction of the displaced intra-articular fracture with minimal surgical trauma.

An anterolateral acromial approach to the proximal humerus has been reported for reduction and fixation of proximal humeral fractures [8–10]. This approach allows direct access to the lateral plating zone and minimizes soft-tissue dissection, which leads to early functional recovery; on the other hand, there is a risk of axillary nerve injury owing to its close anatomical relationship. Our patient showed no complications, such as nonunion, osteonecrosis, or axillary nerve palsy.

In conclusion, we report a patient with posterior fracture–dislocation involving the articular surface. Arthroscopically assisted MIPO provides accurate reduction and stable fixation with minimal surgical trauma, with excellent clinical results.

Conflict of interest The author did not receive any outside funding or grants and has no commercial associations that might pose a conflict of interest in connection with the submitted article.

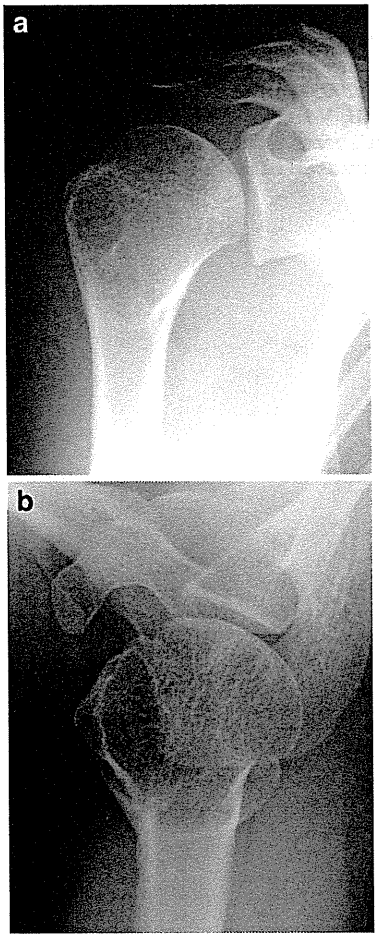

Fig. 5 Postoperative radiographs in anteroposterior (**a**) and axillary (**b**) views at follow-up 15 months after the operation

References

1. Lau TW, Leung F, Chan CF, Chow SP. Minimally invasive plate osteosynthesis in the treatment of proximal humeral fracture. Int Orthop. 2007;31:657–64.
2. Neer CS 2nd. Displaced proximal humeral fractures. I. Classification and evaluation. J Bone Joint Surg Am. 1970;52:1077–89.
3. Robinson CM, Akhtar A, Mitchell M, Beavis C. Complex posterior fracture-dislocation of the shoulder. Epidemiology, injury patterns, and results of operative treatment. J Bone Joint Surg Am. 2007;89:1454–66.
4. Hersche O, Gerber C. Iatrogenic displacement of fracture-dislocations of the shoulder. A report of seven cases. J Bone Joint Surg Br. 1994;76:30–3.
5. Lee CK, Hansen HR. Post-traumatic avascular necrosis of the humeral head in displaced proximal humeral fractures. J Trauma. 1981;21:788–91.
6. Leyshon RL. Closed treatment of fractures of the proximal humerus. Acta Orthop Scand. 1984;55:48–51.
7. Wijgman AJ, Roolker W, Patt TW, Raaymakers EL, Marti RK. Open reduction and internal fixation of three and four-part fractures of the proximal part of the humerus. J Bone Joint Surg Am. 2002;84-A:1919–25.

8. Gardner MJ, Griffith MH, Dines JS, Briggs SM, Weiland AJ, Lorich DG. The extended anterolateral acromial approach allows minimally invasive access to the proximal humerus. Clin Orthop Relat Res. 2005;434:123–9.
9. Gardner MJ, Voos JE, Wanich T, Helfet DL, Lorich DG. Vascular implications of minimally invasive plating of proximal humerus fractures. J Orthop Trauma. 2006;20:602–7.
10. Röderer G, Erhardt J, Graf M, Kinzl L, Gebhard F. Clinical results for minimally invasive locked plating of proximal humerus fractures. J Orthop Trauma. 2010;24:400–6.

Prosthetic limb salvage surgery for bone and soft tissue tumors around the knee

RUI NIIMI, AKIHIKO MATSUMINE, TAKAHIKO HAMAGUCHI, TOMOKI NAKAMURA, ATSUMASA UCHIDA and AKIHIRO SUDO

Department of Orthopaedic Surgery, Mie University Graduate School of Medicine, Mie 514-8507, Japan

Received February 20, 2012; Accepted April 9, 2012

DOI: 10.3892/or.2012.2021

Abstract. In this study, we analyzed long-term survival, limb function and associated complications after prosthetic limb salvage treatment in patients with bone and soft tissue tumors around the knee joint. A total of 63 patients treated with prosthetic limb salvage surgery around the knee were reviewed. The bone tumors involved the distal femur in 45 patients, the proximal tibia in 14 patients and the soft tissue tumors of the proximal lower leg in 4 patients. The median follow-up period after the first operation was 8.0 years. The medical records of the patients, surgical reports, radiographs and histological specimens were retrospectively reviewed. The 5-year overall survival rate was 63.2% in the patients with distal femur tumors and 86.2% in those with tumors of the proximal lower leg. The 5-year prosthetic survival rate was 72.8% in the distal femur and 74.6% in the proximal lower leg. The mean functional score according to the scoring system of the Musculoskeletal Tumor Society (MSTS) was 81% in the patients with distal femur tumors and 82% in the patients with proximal lower leg tumors. Post-operative complications occurred in 27 patients. Limb salvage surgery is considered to be an effective treatment option. However, the high complication rate is a major concern for prosthetic replacement. Future improvements of prostheses are very important.

Introduction

A few decades ago, the primary aim of treatment for sarcoma arising in the extremities was to save the patient's life. Amputation was the standard surgical treatment for musculoskeletal sarcomas of the extremities. In the 1980s, advances in adjuvant therapy improved the tumor control and patient survival, advances in diagnostic imaging allowed more accurate tumor staging and advances in surgical and reconstructive techniques provided limb salvage surgery as a safe alternative to amputation. Today, limb salvage surgery is performed in 70-95% of all patients with bone and soft tissue sarcoma of the extremities, even if the tumor is high-grade (1-4).

However, reconstruction of a large bone defect after resection of a tumor with a wide margin remains a major challenge. The options for reconstruction after resection of a tumor around the knee joint include implantation of a prosthesis, osteoarticular allograft, allograft-prosthesis composite, recycled autologous bone graft, arthrodesis with intercalary bone grafting or conversion to a rotationplasty (5). Prosthetic replacement after resection of a bone tumor around the knee joint has been demonstrated to provide good function in most cases. However, unfortunately, prosthesis-related complications still remain an unresolved problem. Improvement in patient survival has led to subsequent surgical revisions of the prosthesis as a result of increases in prosthesis-related complications. These include periprosthetic infections, aseptic loosening, and wear of the joint components, dislocations, breakage of the prosthesis and fatigue fractures. The long-term functional outcome of the affected limbs depends on these complications. Until now, these are some reports concerning to the prosthetic limb salvage surgery around the knee.

The purpose of this study was to evaluate the clinical and functional results of patients who underwent a limb salvage surgery for tumors around the knee.

Materials and methods

Between 1982 and 2008, 63 patients underwent limb salvage surgery. The mean follow-up period was 8.0 years (range, 0.8-28 years) after the initial operation. The patients' medical records, surgical reports, radiographs and pathologic records were retrospectively reviewed (Table I). Written informed consent was obtained from all of the patients included in this study.

The patient group included 34 males and 29 females, with a mean age of 29 years (range, 11-79 years) at the initial treatment. The bone tumors involved the distal femur in 45 patients, the proximal tibia in 14 patients, and the soft tissue tumors of the proximal lower leg in 4 patients. There were 45 high-grade osteosarcomas (OS), 3 chondrosarcomas, 3 malignant fibrous histiocytomas (MFH), 5 giant cell tumors (GCT) and other in 7 patients. According to the Enneking

Correspondence to: Dr Akihiko Matsumine, Department of Orthopaedic Surgery, Mie University Graduate School of Medicine, 2-174 Edobashi, Tsu, Mie 514-8507, Japan
E-mail: matsumin@clin.medic.mie-u.co.jp

Key words: sarcoma, knee joint, reconstruction, function, complications

staging system (6), one patient was categorized as Stage I, four patients as IIA, 50 patients as IIB, and three patients as III. The surgical excisions were performed with wide margins in all cases. Forty-six patients underwent chemotherapy pre- and post-operatively. The chemotherapy was performed using a combination of 2-4 chemotherapeutic drugs, including cisplatin, doxorubicin, cyclophosphamide, ifosfamide and methotrexate. Post-operative chemotherapy was started 2-3 weeks after surgery. No patient underwent radiotherapy.

Surgical methods. The surgical technique involved resection of the tumor and reconstruction of the knee joint. The biopsy root was also excised *en bloc* with a margin of >3-cm in the malignant lesion. The tumor resection was carried out according to standard oncologic principles. In all cases, the surgical excision was performed with a wide margin (5). In the distal femoral tumors, the median resection length was 16 cm (range, 9-22 cm), and in the proximal tibia tumors, the median resection length was 14 cm (range, 11-21 cm).

Special attention was given to cover the prosthesis completely with muscle tissue. For the distal femur tumors, the remaining vastus medialis was sutured to the rectus femoris. The sartorius muscle could be mobilized and rotated anteriorly for additional closure of the remaining medial soft tissue defect. For the proximal lower leg tumor, reconstruction of the extensor mechanism was performed in all patients. The patellar tendon and anterior capsule were advanced and sutured to the anterior aspect of the prosthesis using unabsorbent thread. A medial gastrocnemius transposition flap (GTF) was used in all cases to provide adequate soft-tissue coverage. In one patient, suturing of the patellar ligament to the anteriorly transferred fibula was performed, and this was then followed by covering the prosthesis with a GTF.

Prosthesis. After resection of the tumor, reconstruction was performed using a prosthesis. Depending on the year the surgery was performed four types of prostheses were used, which were selected depending on the tumor location. From 1982 to 1987, a custom-made prosthesis manufactured by Nemoto-shokai (Tokyo, Japan) was used. This prosthesis has a restrained hinge and was fixed with cement. Three Nemoto-shokai custom-made prostheses were used for reconstruction of distal femurs and six were used for proximal lower legs. From 1988 to 1997, cementless prostheses, HMRS (Stryker-Howmedica-Osteonics, Rutherford, NJ), were used for reconstruction of distal femurs. Thirteen HMRS prostheses were used for reconstruction of distal femurs. This type of prosthesis is still being used for the proximal lower leg. In all 12 HMRS prostheses were used for proximal lower legs during the study period. The HMRS is a first-generation modular endoprosthetic system. It features intramedullary, cementless, press-fit stems supported by external flanges and cortical transfixation screws. The knee mechanism consists of a simple hinge design. From 1997, for the reconstruction of the distal femur, 26 patients were treated using the KLS/PHKIII system (Japan Medical Materials, Osaka, Japan). The KLS/PHKIII is an original prosthesis in that the metallic parts are fully made of titanium alloy, and this prosthesis has a unique semi-rotating hinge joint and was designed especially for people with the Asian body type/stature (7). Three patients with distal femur tumors were implanted with other types of modular prostheses in the 1980s.

Table I. Details of the patient characteristics.

	Distal femur (45 patients)	Proximal tibia (18 patients)
Age	30 (11-79)	28 (13-68)
Gender		
Male	25	9
Female	20	9
Follow-up periods (months)	78.3 (3-340)	141 (5-305)
Diagnosis[a]		
OS	35	10
MFH	1	2
Metastasis	2	1
CS	3	0
GCT	4	1
Others	0	4
Surgical staging[b]		
3	4	1
IA	0	1
IIA	4	0
IIB	34	16
III	3	0
Prosthesis		
Custom made	3	6
Modular	42	12

[a]OS, osteosarcoma; MFH, malignant fibrous histiocytomas; CS, chondrosarcoma; GCT, giant cell tumor. [b]Stage 3 is gengin aggresive lesion; Stage IA is a low-grade, intracompartmental lesion without metastases; Stage IB is a low-grade, extracompartmental lesion without metastases; Stage IIA is a high-grade, intracompartmental lesion free of metastases; Stage IIB is a high-grade, extracompartmental lesion without metastases; and Stage III is setting with metastases.

Assessment and statistical analysis. The oncological results, functional results, and complications were investigated. A functional evaluation was performed using the scoring system of the Musculoskeletal Tumor Society (MSTS) which consists of six parameters (pain, function, use of walking aids, walking activity, gait and emotional acceptance) (8). The actuarial data for the overall survival rate, disease-free survival rate, prosthesis survival rate and limb salvage rate at the final follow-up were calculated using a Kaplan-Meier analysis. The prosthesis survival rate was calculated as the time from the surgical reconstruction using the prosthesis to revision or amputation due to prosthetic failure. Prosthetic failure was defined as replacement of any parts of the prosthetic components, including minor parts of the prosthesis due to local tumor recurrence, polyethylene bushing failures, breakage of the prosthesis and aseptic loosening or infection. Log-rank analyses were used to determine the factors which influenced the prosthesis survival rate. The factors included tumor locations, patient ages (<30

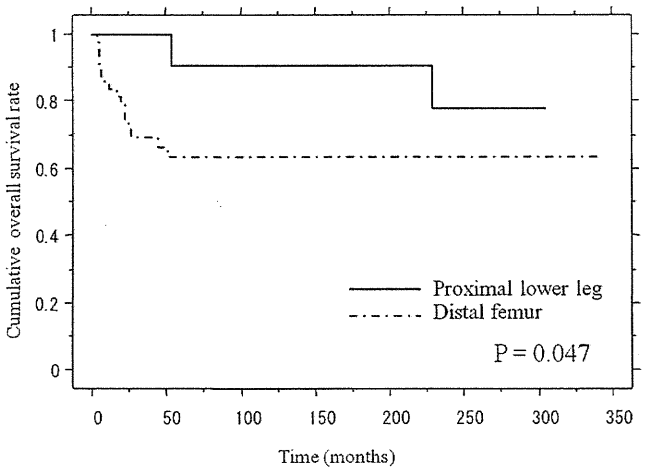

Figure 1. Cumulative overall survival of patients with sarcoma around the knee.

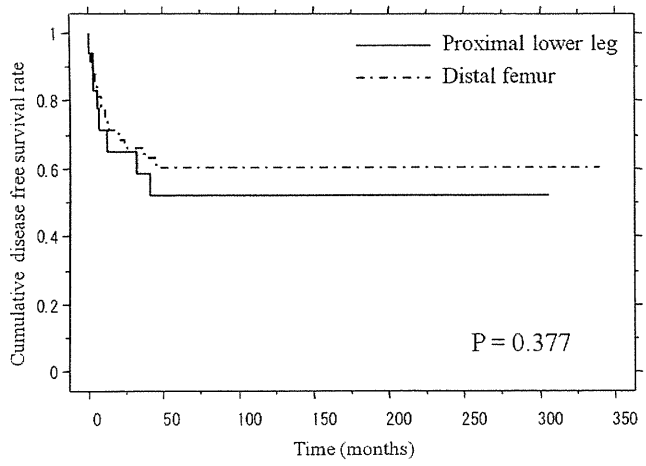

Figure 2. Cumulative disease-free survival of patients with sarcoma around the knee.

vs. ≥30 years), gender, peroneal palsy vs. non-peroneal palsy, extension lag (<30° vs. ≥30°) and primary vs. revision procedures. Mann-Whitney U tests were also used to determine the factors which correlated with the post-operative results of limb function. The factors included tumor locations, patient ages (<30 vs. ≥30 years), gender, perorneal palsy vs. non-peroneal palsy, extension lag (<30° vs. ≥30°) and primary vs. revision procedures. Analyses were performed using the Statview 5.0 software program (SAS Institute, Inc., Cary, NC, USA). A P-value <0.05 was considered to be statistically significant.

Results

Oncological results. At the final follow-up, 36 patients were continuously disease-free, 8 patients had no evidence of disease, two patients alive with disease and 17 were patients dead of disease. The 5-year overall survival rate was 63.2% in the distal femur cases and 86.2% in the proximal lower leg cases. The log-rank test showed that there was a significant difference between the cumulative survival rates based on the tumor location (P=0.047) (Fig. 1). The patients with tumors in their

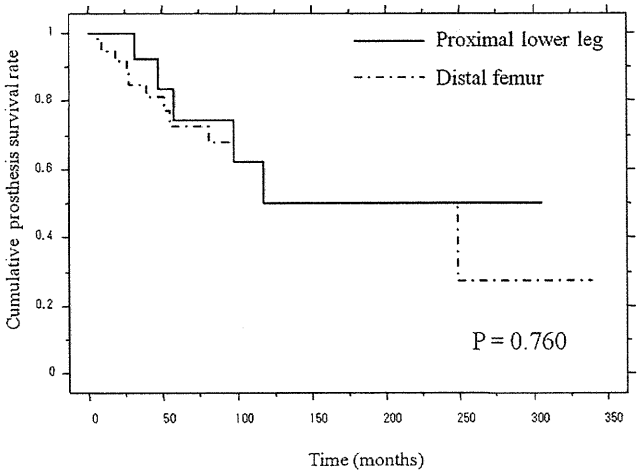

Figure 3. Cumulative prosthetic survival of patients with sarcoma around the knee.

Table II. Results of the univariate analysis showing the factors which affect the 5-year prosthesis survival rate.

Factors	No. of patients	5-year prosthesis survival rate (%)	P-value[a]
Tumor location			
Distal femur	45	72.8	0.76
Proximal tibia	18	74.6	
Age (years)			
<30	31	75.3	0.91
≥30	32	70.3	
Gender			
Male	34	72.1	0.88
Female	29	76.0	
Peroneal nerve palsy			
Yes	13	83.3	0.91
No	50	72.5	
Extension lag			
<30°	13	73.3	0.053
≥30°	4	0	

[a]Log-rank test.

proximal lower legs had a better overall survival rate than those with distal femoral tumors. The 5-year disease-free survival rates were 62.4 and 52.2% in the patients with distal femur and the proximal leg tumors, respectively (Fig. 2). There were no significant differences between the disease-free survival rates with regard to the tumor location (log-rank test, P=0.377).

Prosthetic survival. The 5-year prosthetic survival rate was 72.8% in the distal femur cases and 74.6% in the proximal lower leg cases (Fig. 3). There were no significant differences between the prosthesis survival rates based on the tumor location (log-rank test, P=0.760). During the follow-up period, no limb amputation was performed. The log-rank test showed no statistical difference between the prosthetic survival based on

Table III. Results of the univariate analysis showing the factors which affect the MSTS score.

Factors	No. of patients	MSTS score	P-value[a]
Tumor location			
Distal femur	45	81 (40-100)	0.73
Proximal lower leg	18	82 (53-97)	
Age (years)			
<30	31	81 (37-100)	0.85
≥30	32	82 (40-100)	
Gender			
Male	34	86 (53-100)	0.04
Female	29	75 (37-100)	
Peroneal nerve palsy			
Yes	13	66 (37-97)	0.01
No	50	85 (60-100)	
Extension lag			
<30°	13	91 (73-100)	<0.01
≥30°	4	63 (37-73)	
Primary	46	82 (37-100)	0.89
Revision	17	78 (53-97)	

[a]Log-rank test.

the following factors: patient's age, tumor location, gender, presence of peroneal nerve palsy and the presence of extension lag (Table II).

Functional results. The mean post-operative functional score was 81% (range, 37-100%). The mean functional score was 81% (range, 37-100%) in the patients with distal femur tumors and 82% (range, 53-97%) in the patients with proximal lower leg tumors (Table III).

Regarding the functional results, the Mann-Whitney U test showed that male patients had significantly better limb function than female patients (P=0.04). Patients with peroneal nerve palsy showed significantly worse MSTS scores than those without peroneal palsy (Mann-Whitney U test, P=0.01). Patients with extension lag in excess of 30° had a worse MSTS score than those with less extension lag (P<0.01). The Mann-Whitney U test showed no significant difference in MSTS scores between primary and revision surgery (P=0.89).

Complications. A total of 27 of the 63 patients (43%) developed post-operative complications. Forty-nine post-operative complications occurred in these 27 patients. The major complications were peroneal palsy in 13 patients (21%), followed by loosening in 7 patients (11.1%), breakage of the hinge mechanism in 4 patients (6.3%), breakage of the stem in 4 patients (6.3%), breakage of a femoral or tibial component in 4 patients (6.3%), a leg length discrepancy of >2 cm in 4 patients (6.3%), local recurrence in 4 patients (6.3%), deep infection in 3 patients (4.8%), skin trouble in 3 patients (4.8%), a periprosthetic fracture in 2 patients (3.2%), and secondary cancer after chemotherapy in 1 patient (1.6%) (Table IV).

Table IV. Complications.

	Distal femur (45 patients)	Proximal tibia (18 patients)
Prosthesis-related complications		
Breakage of prosthesis	11	3
Loosening	6	1
Peroneal nerve palsy	5	8
Leg length discrepancy (≥2 cm)	4	0
Recurrence	3	1
Deep infection	1	2
Skin trouble (only superficial)	2	1
Secondary cancer	1	0

Forty-three operations were eventually required to treat these complications. For the deep infections, 19 operations were required, including debridement, primary sutures or coverage with a skin flap. For the skin troubles, 7 minor operations such as secondary suturing were performed. For loosening of the prosthesis, three revision surgeries were required. For the breakage of stems, 4 revision surgeries were performed. Four and 6 surgeries were performed to repair a breakage of a femoral or tibial component, or the breakage of a hinge (e.g., breakage of bush or insert), respectively. Two of the 4 patients with local recurrence underwent a wide excision of the recurrent tumor preserving the prosthesis, and one patient exchanged the prosthesis. Another patient with multiple metastases did not undergo surgery because of a putative poor prognosis.

In cases of distal femoral reconstruction, 6 prostheses, including 3 modular prostheses and 3 custom-made prostheses, were implanted before 1987. Breakage of prosthetic components was observed in 3 of these 6 prostheses (50%). Three patients had 4 breakages of their prosthesis. One patient experienced the breakage of a stem. One patient had loosening of a component. One patient had breakage of the hinge after breakage of the stem. But since the HMRS or KLS/PHK III were introduced for reconstruction, the rate of prosthesis breakage was 23% (9 of 39 prostheses). Nine patients had 13 breakages of the prosthesis.

In addition, in the 6 cases of proximal tibial reconstruction using custom-made prostheses which were implanted before 1987, breakage of the prosthesis was observed in 2 cases (33%). One patient had breakage of a tibial component, and the other patient had loosening of the prosthesis. But since the HMRS was introduced for reconstruction, the rate of prosthesis breakage has been 17% (2 of 12 patients). One patient suffered the breakage of both the bush and tibial components two times, while another patient had breakage of a tibial component.

Discussion

In this study, the 5-year overall survival rate was 63% in the patients with distal femur tumors and 86% in those with tumors of the proximal lower leg. The 5-year disease-free